*reactions*

MDPI

*Communication*

# Increased Yields of the Guanine Oxidative Damage Product Imidazolone Following Exposure to LED Light

**Taishu Kawada [1], Moka Maehara [2] and Katsuhito Kino [2,3,*]**

[1] Kagawa School of Pharmaceutical Sciences, Tokushima Bunri University, 1314-1 Shido, Sanuki-shi 769-2193, Kagawa, Japan; s108019@stu.bunri-u.ac.jp
[2] Faculty of Science and Engineering, Tokushima Bunri University, 1314-1 Shido, Sanuki-shi 769-2193, Kagawa, Japan; s215620@stu.bunri-u.ac.jp
[3] Center for Advance Science and Engineering (CASE), Tokushima Bunri University, 1314-1 Shido, Sanuki-shi 769-2193, Kagawa, Japan
* Correspondence: kkino@kph.bunri-u.ac.jp; Tel.: +81-87-899-7290

**Abstract:** Among the bases of DNA, guanine is the most easily oxidized. Imidazolone (Iz) is a guanine oxidative damage, and we sought to generate Iz-containing oligomers. In this paper, we describe the methods and conditions to increase the yield of Iz by employing photooxidation reactions using light-emitting diodes (LEDs) with emission wavelengths of 365 nm and 450 nm. For photooxidation performed with the 450 nm LED source at light intensities of 2.75–275 mW/cm$^2$, peak yields of Iz were 35% at light intensities of 27.5 and 68.8 mW/cm$^2$. For reactions performed with the 365 nm LED source at light intensities of 5.12–512 mW/cm$^2$, the peak yield of Iz was 34% at a light intensity of 51.2 mW/cm$^2$. By varying the irradiation time, the maximum yield of Iz (34–35%) was obtained with irradiation times of 5–20 min using the 450 nm LED source at an intensity of 13.8 mW/cm$^2$. Using the 365 nm LED source at an intensity of 25.6 mW/cm$^2$, the maximum Iz yield obtained was 31% at irradiation times of 2–5 min. Thus, we obtained conditions that can provide an Iz yield of up to 35%.

**Keywords:** guanine oxidative damage; light irradiation; flavin; LED



**Citation:** Kawada, T.; Maehara, M.; Kino, K. Increased Yields of the Guanine Oxidative Damage Product Imidazolone Following Exposure to LED Light. *Reactions* **2023**, *4*, 801–810. https://doi.org/10.3390/reactions4040046

Academic Editor: Dmitry Yu. Murzin

Received: 20 October 2023
Revised: 13 November 2023
Accepted: 12 December 2023
Published: 16 December 2023



## 1. Introduction

DNA is oxidized by ultraviolet light, radiation, reactive oxygen species, and light irradiation in the presence of photosensitizers [1–24]. Oxidized DNA is one of the factors that cause mutations leading to cancer. Among the four bases of DNA, guanine, which has the lowest oxidation potential [25], is the most susceptible to oxidation [26–29], meaning that, among oxidative lesions, guanine oxidative damage is the most likely to occur.

Among guanine oxidative damage events, 8-oxoguanine (8-oxoG) is one of the earliest-detected lesions that has a biological impact [30–33] and is known to contribute to G:C→T:A transversions but not to G:C→C:G transversions [34–36]. Therefore, guanine oxidative damage other than 8-oxoG may be involved in G:C→C:G transversions. Guanine oxidative lesions such as imidazolone (Iz) (Figure 1) [37,38], oxazolone (Oz) (Figure 1) [37,38], guanidinohydantoin (Gh) [39,40], and spiroiminohydantoin (Sp) [39–41] have been reported to contribute to G:C→C:G transversions [42–50]. The structures of both Gh and Sp have sp$^3$ carbons that break the π-π stacking of DNA. On the other hand, Iz and Oz have planar structures and are more favorable for DNA elongation than Gh and Sp [44,46]. Moreover, since Iz is gradually degraded to Oz under in vivo conditions, we believe that Iz and Oz are important for the generation of point mutations in human cells.

To build on these previous in vitro studies on Iz and Oz, it is necessary to clarify whether Iz/Oz-induced mutations occur in cells. Such analyses require the preparation of large quantities of DNA oligomers containing Iz, and we thought that using a light source with higher intensity than a transilluminator for one-electron photooxidation would

increase the efficiency of the photoreaction, and then increase the yield of Iz. When irradiated with demonstration equipment from various companies including a laser, the yield of Iz increased with devices that emit light with a stronger intensity than a transilluminator. However, with too strong light irradiation, the raw material was completely lost, and the yield of Iz was lower than that when irradiated with a transilluminator. Therefore, it has become necessary to perform an analysis using a light irradiation device that can vary the intensity. In addition, recently, photochemical synthesis using light-emitting diode (LED) has been reported [51–58]; LED sources are cheap and easily available. Therefore, we chose LED as the irradiation device to reduce the cost for Iz generation. As shown below, we conducted photoreactions with a previously used ultraviolet (UV) transilluminator and newly purchased LED sources, and then examined the conditions under which Iz can be generated efficiently. Notably, DNA 30-mers containing Iz (5′-CTCATCAACATCTTIzAATTCACAATCAATA-3′), the substrate that we use in our polymerase analysis, are difficult to separate by high-performance liquid chromatography (HPLC). Therefore, we instead employed DNA 6-mers (5′-CTTXAA-3′, where X is guanine or Iz), for which HPLC can be used to separate the guanine- and Iz-containing oligomers. The 6-mers containing DNA damage products were then used to synthesize DNA 30-mers using a previously described ligation method.

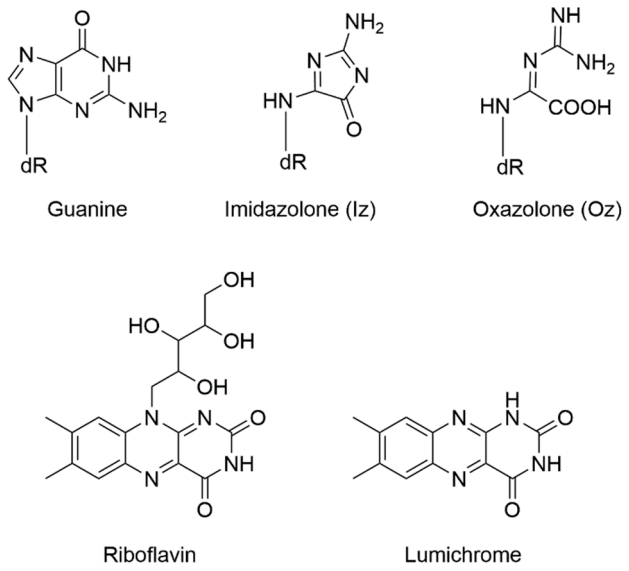


**Figure 1.** The structures of guanine, imidazolone (Iz), oxazolone (Oz), riboflavin and lumichrome.

## 2. Materials and Methods

Riboflavin (Figure 1) was purchased from Kishida Chemical Co., Ltd. (Osaka, Japan). The 6-mer oligonucleotide (5′-CTTGAA-3′) was purchased from Japan Bio Service Co., Ltd. (Saitama, Japan). The reaction solution consisted of 10 μM 5′-CTTGAA-3′, 75 μM riboflavin, and 5 mM cacodylate buffer (pH 7.0). In Figure 2, photoreactions employed a 3UV™ Transilluminator (Model LMS-26E; UVP LLC, Upland, CA, USA; 6.5 mW/cm$^2$) for 1–120 min. A controller (Model CL-1501) and LED sources with emission wavelengths of 365 nm (Model CL-H1-365-9-1-B; 512 mW/cm$^2$) and 450 nm (Model CL-H1-450-9-1-B; 275 mW/cm$^2$) were purchased from Asahi Spectra Co., Ltd. (Tokyo, Japan), and these LED sources were used in the experiments presented in Figures 3 and 4. The distance between the light source and the reaction solution was set to 4 cm in Figures 2–4. Figure 3 shows a solution that was irradiated for 2 min with the 450 nm LED with light intensities of 2.75, 13.8, 27.5, 68.8, 138, 206, and 275 mW/cm$^2$ or the 365 nm LED with light intensities of 5.12, 25.6, 51.2, 128, 256, and 512 mW/cm$^2$. Figure 4 shows a solution that was irradiated for 2–20 min with the 450 nm LED with an intensity of 13.8 mW/cm$^2$ or the 365 nm LED with an intensity of 25.6 mW/cm$^2$. Photo-reacted solutions were analyzed by HPLC using a

CHEMCOBOND 5-ODS-H column (Chemco Plus Scientific Co., Ltd., Osaka, Japan); 5 µm, 150 × 4.6 mm; solvent: 50 mM TEAA (pH 7.0), 7–9% $CH_3CN$; cycle length: 30 min; flow rate: 1.0 mL/min), and absorbance was monitored at 260 nm. Identification of DNA 6-mers containing Iz was performed as described previously [5,42].

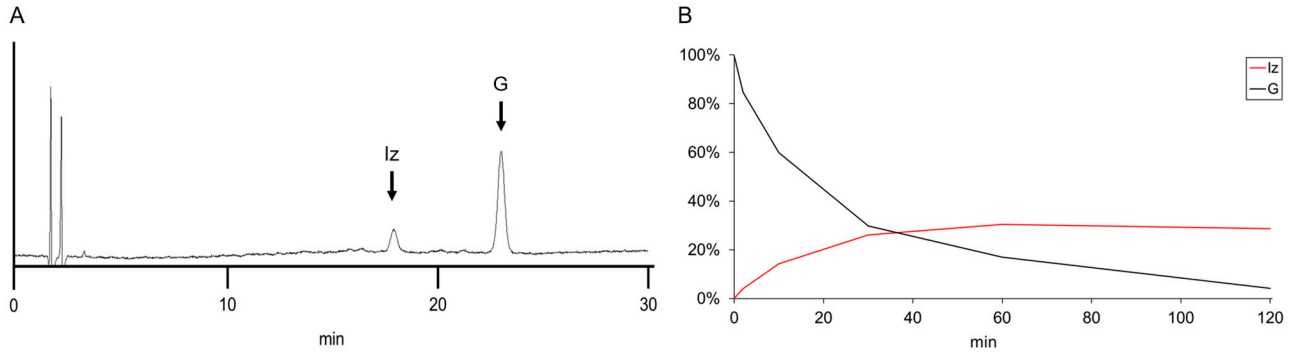


**Figure 2.** Photooxidation of guanine-containing DNA oligomers under UV-A irradiation with a transilluminator. (**A**) A representative spectrogram showing the results of HPLC analysis of the solution subjected to photooxidation for 10 min. "G" is 5′-CTTGAA-3′. "Iz" is 5′-CTTIzAA-3′. (**B**) Time course of photooxidation. The graph shows the percentages of the raw material remaining (black line) and the percentages of Iz produced (red line); the amount of the raw material at baseline (before photoirradiation) was defined as 100% (on the y-axis). Analyses were performed twice, and the mean was calculated.

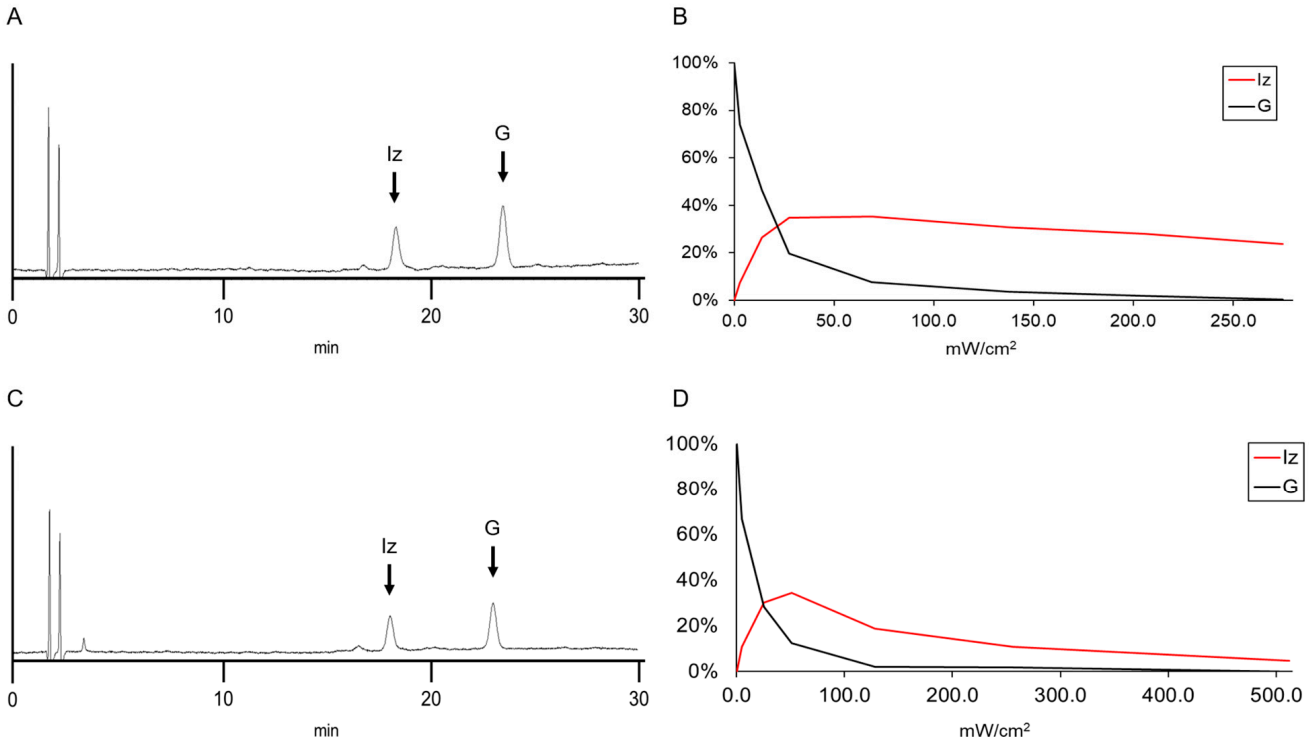


**Figure 3.** Photooxidation of guanine-containing DNA oligomers under irradiation with an LED source at various light intensities. A solution was irradiated for 2 min with 450 nm (**A**,**B**) or 365 nm (**C**,**D**) light from an LED source. (**A**) A representative spectrogram showing the results of HPLC analysis of the solution subjected to photooxidation with the 450 nm light at an intensity of 13.8 mW/cm$^2$. "G" is 5′-CTTGAA-3′. "Iz" is 5′-CTTIzAA-3′. (**C**) A representative spectrogram showing the results of HPLC analysis of the solution subjected to photooxidation with the 365 nm light at an intensity of

25.6 mW/cm$^2$. (**B**,**D**) Photooxidation at various light intensities. The graphs show the percentages of the raw material remaining (black line) and the percentage of Iz produced (red line); the amount of the raw material at baseline (before photoirradiation) was defined as 100% (on the y-axis). Analyses were performed twice, and the mean was calculated.

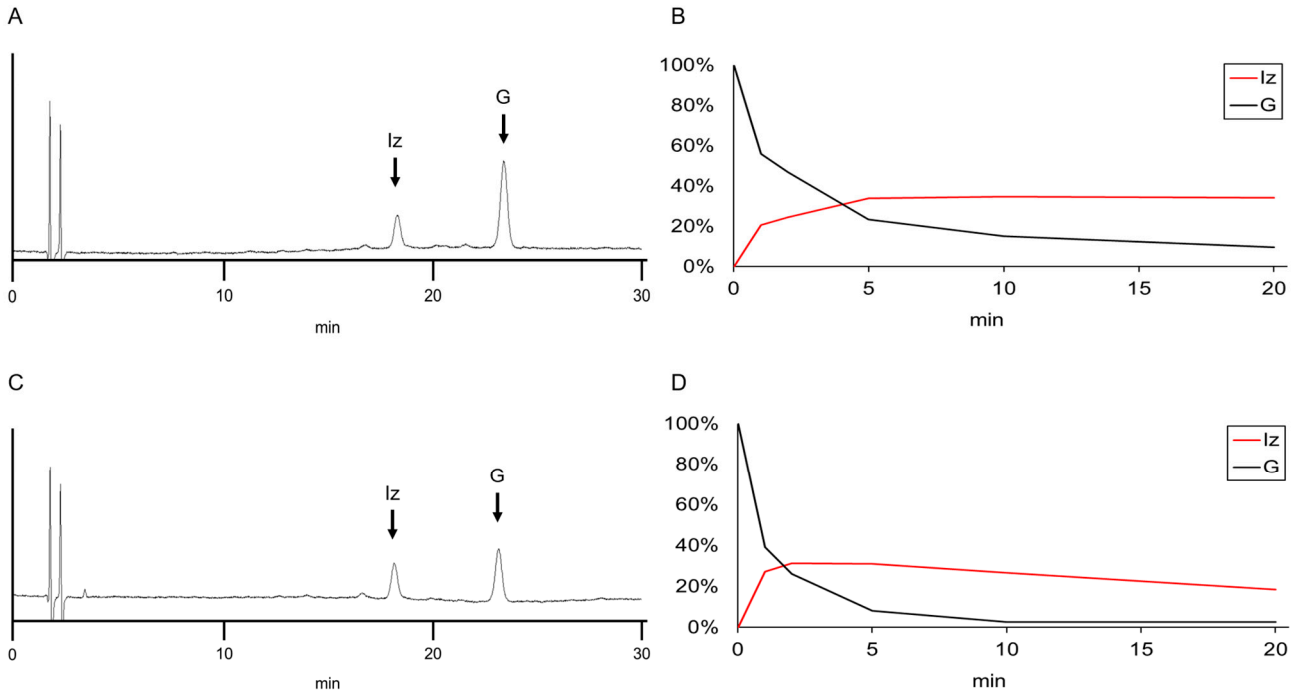


**Figure 4.** Photooxidation of guanine-containing DNA oligomers under irradiation with an LED source for various reaction times. A solution was irradiated for various intervals with the 450 nm light at an intensity of 13.8 mW/cm$^2$ (**A**,**B**) or with the 365 nm light at an intensity of 25.6 mW/cm$^2$ (**C**,**D**) using an LED source. (**A**,**C**) A representative spectrogram showing the results of HPLC analysis of the solution subjected to photooxidation (1 min) with 450 nm (**A**) or 365 nm (**C**) light. "G" is 5′-CTTGAA-3′. "Iz" is 5′-CTTIzAA-3′. (**B**,**D**) Time course of photooxidation. The graphs show the percentages of the raw material remaining (black line) and the percentage of Iz produced (red line); the amount of the raw material at baseline (before photoirradiation) was defined as 100% (on the y-axis). Analyses were performed twice, and the mean was calculated.

## 3. Results and Discussion

### *3.1. Reanalysis of Iz Generation Using Transilluminator*

Since guanine has the lowest oxidation potential in DNA [25], one-electron oxidation of guanine with excited riboflavin leads to the generation of Iz [37–39,42–45]. Taking advantage of this property, DNA oligomers containing single Iz can be synthesized from DNA oligomers containing single guanine. In our laboratory, the Iz-containing product (5′-CTTIzAA-3′) previously was generated from the raw material (5′-CTTGAA-3′) using a UVP transilluminator. To compare with LED-based photoreactions (described below), transilluminator-based photoreactions were repeated as part of the current study. The raw material was irradiated with 365 nm light in the presence of riboflavin, and the distance between the light source and the reaction solution was set to 4 cm. When the quantity of the raw material before light irradiation was set to 100%, the calculated yields of Iz at various irradiation times were as follows: 4% at 2 min, 14% at 10 min, 26% at 30 min, 30% at 60 min, and 29% at 120 min (Figure 2). The yield of Iz following irradiation for 120 min did not increase compared to that obtained at 60 min, so the irradiation was not performed for intervals exceeding 120 min.

### *3.2. Analysis of Iz Yields Using LEDs at Various Light Intensities*

Next, to increase the yield of Iz, we used two LEDs (purchased from Asahi Spectroscopy, Tokyo, Japan), for which the irradiation light intensity (maximum light intensities of 512 and 275 mW/cm$^2$ at 365 and 450 nm) exceed that provided by the UVP transilluminator (6.5 mW/cm$^2$). Given that blue-light irradiation in the presence of riboflavin leads to the production of Iz from deoxyguanine [59,60], as well as the observation that riboflavin has two absorption maxima (at 360–380 nm and 440–450 nm) [61–67], we selected LED sources with emission wavelengths of 365 and 450 nm for the experiments described here.

Photoreactions were performed using the 450 nm LED while adjusting the irradiation light intensity from 0 to 275 mW/cm$^2$ (Figure 3A,B). The Iz yields at various light intensities were as follows: 8% at 2.75 mW/cm$^2$, 27% at 13.8 mW/cm$^2$, 35% at 27.5 mW/cm$^2$, 35% at 68.8 mW/cm$^2$, 31% at 138 mW/cm$^2$, 28% at 206 mW/cm$^2$, and 24% at 275 mW/cm$^2$ (Figure 3B). Thus, peak Iz yields (35%) were obtained at light intensities of both 27.5 and 68.8 mW/cm$^2$. Using LED sources with a stronger intensity than that of a transilluminator increased the efficiency of the photoreaction, resulting in an increase in the yield of Iz. However, the Iz yields at light intensities exceeding 138 mW/cm$^2$ were lower than the maximum yield (Figure 3B).

Using the 365 nm LED source under the same conditions, the Iz yields obtained at various light intensities were as follows: 11% at 5.12 mW/cm$^2$, 30% at 25.6 mW/cm$^2$, 34% at 51.2 mW/cm$^2$, 19% at 128 mW/cm$^2$, 11% at 256 mW/cm$^2$, and 5% at 512 mW/cm$^2$ (Figure 3D). Therefore, the peak Iz yield (34%) was obtained at a light intensity of 51.2 mW/cm$^2$; this value was nominally lower than the peak obtained using the 450 nm LED source (Figure 3D). The Iz yield decreased at light intensities exceeding 51.2 mW/cm$^2$ (Figure 3D). These results indicated that, for LED sources, peak light intensity did not provide peak production of Iz, an observation that is discussed further in Section 4.

### *3.3. Analysis of the Efficiency of Iz Generation at Various LED Irradiation Times*

The results obtained using the transilluminator indicated that the yield of Iz did not increase when changing the irradiation time from 60 to 120 min (Figure 2). However, given the results of the high irradiation light intensity provided by the LED sources (Figure 3), it was possible that the yield of Iz decreased with the increase in LED irradiation time. To test this hypothesis, we repeated our experiments using various time intervals for irradiation with LED sources at fixed light intensities of either 13.8 mW/cm$^2$ at 450 nm or 25.6 mW/cm$^2$ at 365 nm. We then quantified the yield of Iz at each irradiation time point (Figure 4).

For the 450 nm LED source, photoreactions were performed at intervals of 0–20 min. The Iz yields at various times were as follows: 21% at 1 min, 24% at 2 min, 34% at 5 min, 35% at 10 min, and 34% at 20 min (Figure 4B). The Iz yield fell to 23% after irradiation for 60 minutes (Figure S1). Thus, the Iz yield peaked at 34–35% with irradiation intervals of 5–20 min and decreased with longer intervals of irradiation.

For the 365 nm LED source, photoreactions were performed for intervals of 0–20 min. The Iz yields at various times were as follows: 27% for 1 min, 31% at 2 min, 31% at 5 min; 27% at 10 min, and 18% at 20 min (Figure 4D). Therefore, the peak Iz yield was 31% at 2–5 min, and decreased with longer intervals of irradiation. We suggest a possible reason for this decrease in Iz yield in Section 4.

### *3.4. Exploring Why the Yield of Iz Decreases at Higher Light Intensities or Longer Irradiation Times*

In Sections 2 and 3, we noted that, with LED irradiation (at either 450 nm or 365 nm), longer irradiation times and stronger light intensity conditions resulted in decreased product yields. To investigate the basis of this phenomenon, we used an alternative oligonucleotide (5′-CTTCAA-3′) that does not contain guanine; this reactant was subjected to 2 min of irradiation with the 365 nm LED at an intensity of 51.2 mW/cm$^2$. Under these conditions, 22% of the raw material was converted (Figure S2); in contrast, 88% of

oligomers containing guanine was converted under the same conditions (Figure 3D). Thus, oligomers lacking guanine still underwent photoreaction, although the yield was decreased compared to that observed with oligomers containing guanine; we inferred that excessive light irradiation decomposes the product.

Riboflavin is capable of oxidizing guanine upon irradiation with light of a wavelength of 365 or 440 nm [59,60], simultaneously undergoing degradation to produce lumichrome (Figure 1) [59,60,68–74]. Lumichrome absorbs light at 365 nm but not at 440 nm; therefore, unlike the case with 365 nm light, irradiation with 440 nm light in the presence of lumichrome will not oxidize guanine [59,60]. Even when the oligonucleotide (5′-CTTGAA-3′) was used, it did not react with 450 nm light in the presence of lumichrome but reacted with 366 nm light to generate Iz (Table S1). Thus, the difference in the results seen for irradiation at 450 and 365 nm in Figures 3 and 4 (respectively) may reflect the difference in the photooxidative capacities of riboflavin and lumichrome. To permit determination of the contribution of the photosensitizer, the HPLC gradient was changed to 7–30% $CH_3CN$ over 30 min, and the levels of riboflavin and lumichrome were quantified at 365 nm (Figure S3).

Under the conditions employed in Figure 3, irradiation with 450 nm light at an intensity of 27.5 mW/cm$^2$ resulted in riboflavin at 59% of the input concentration, with a yield of 13% lumichrome. On the other hand, irradiation with the 450 nm light at an intensity of 275 mW/cm$^2$ resulted in riboflavin at 5% of the input concentration, with a yield of 39% lumichrome. These results indicated that riboflavin persists in greater amounts than lumichrome under the conditions that provide the highest yield of Iz, while riboflavin is largely eliminated under conditions that decrease the yield of Iz. Similar results were seen for photooxidation with 365 nm light; irradiation at a light intensity of 51.2 mW/cm$^2$ yielded 39% riboflavin and 21% lumichrome, while irradiation at 512 mW/cm$^2$ yielded 1% riboflavin and 18% lumichrome.

Under the conditions employed in Figure 4, five minutes of irradiation with 450 nm light yielded riboflavin and lumichrome at 61% and 13%, respectively; twenty minutes of irradiation with 450 nm light yielded values of 20% and 32%. Five minutes of irradiation with 365 nm light yielded riboflavin and lumichrome at 39% and 22%, respectively; twenty minutes of irradiation with 365 nm light yielded values of 6% and 39%. These results resembled those described in the preceding paragraph for experiments performed under the conditions used in Figure 3.

Thus, our results suggested that, for irradiation with 365 nm light, lumichrome (a photoproduct of riboflavin) serves as a photosensitizer even upon the depletion of riboflavin, and Iz yield is decreased under conditions of stronger light intensity or prolonged irradiation (Figures 3D and 4D). On the other hand, for irradiation with 450 nm light, photogenerated lumichrome does not act as a photosensitizer; only the remaining riboflavin contributes to a decrease in Iz concentration, and this decrease occurs more slowly than that seen at 365 nm (Figures 3B and 4B).

## 4. Conclusions

DNA oligomers containing Iz are synthesized more efficiently using irradiation with LED sources emitting light at 365 nm (at a light intensity of 512 mW/cm$^2$) or 450 nm (at a light intensity of 275 mW/cm$^2$) than a transilluminator (at a light intensity of 6.5 mW/cm$^2$), which is the previously described technique. By optimizing the light intensity and the interval of irradiation time, the yield of Iz was increased to 35%, as obtained using an LED light at 450 nm.

Although Iz gradually degrades under in vivo conditions, Iz is an important DNA damage because it may have more of an effect on metabolically active cells such as cancer cells than on normal cells. The results of this study showed that more Iz was obtained in a shorter time by LEDs than by a transilluminator, making it easier to use Iz as a research material. In addition, a large amount of Oz can be obtained by decomposing Iz, which is useful for research on Oz.

**Supplementary Materials:** The following supporting information can be downloaded at: https://www.mdpi.com/article/10.3390/reactions4040046/s1, Figure S1: Photooxidation of guanine-containing DNA oligomers under irradiation with a LED light source for 60 min. "*" was not derived from DNA; Figure S2: Photooxidation of cytosine-containing DNA oligomers under irradiation with a LED light source at an intensity of 51.2 mW/cm$^2$. HPLC analysis (260 nm) of reaction solution after (A) no and (B) 2 min of irradiation. "*" was not derived from DNA. Figure S3: Photooxidation of riboflavin under irradiation with a LED light source for various reaction times. A solution was irradiated for various intervals with 450-nm light at an intensity of 13.8 mW/cm$^2$ (A) or with 365-nm light at an intensity of 25.6 mW/cm$^2$ (B). Table S1: Photooxidation of guanine-containing DNA oligomers under irradiation with two LED light sources. The reaction solution consisted of 10 μM 5′-CTTGAA-3′, 75 μM lumichrome, and 5 mM cacodylate buffer (pH 7.0)/0.84% DMSO.

**Author Contributions:** Conceptualization, K.K.; validation, T.K. and K.K.; formal analysis, T.K. and K.K.; investigation, T.K., M.M. and K.K.; resources, T.K. and K.K.; data curation, T.K., M.M. and K.K.; writing—original draft preparation, T.K. and K.K.; writing—review and editing, T.K., M.M. and K.K.; visualization, T.K. and K.K.; supervision, K.K.; project administration, K.K.; funding acquisition, K.K. All authors have read and agreed to the published version of the manuscript.

**Funding:** Our research is supported by JSPS KAKENHI 17K00558 and 23K11427.

**Data Availability Statement:** The authors confirm that the data supporting the findings of this study are available within the article.

**Acknowledgments:** Thank you for the administrative support of Tokushima Bunri University.

**Conflicts of Interest:** The authors declare no conflict of interest. The funders had no role in the design of the study; in the collection, analyses, or interpretation of data; in the writing of the manuscript; or in the decision to publish the results.

## References

1. Negishi, K.; Hao, W. Spectrum of mutations in single-stranded DNA phage M13mp2 exposed to sunlight: Predominance of G-to-C transversion. *Carcinogenesis* **1992**, *13*, 1615–1618. [CrossRef]
2. Takimoto, K.; Tano, K.; Hashimoto, M.; Hori, M.; Akasaka, S.; Utsumi, H. Delayed transfection of DNA after riboflavin mediated photosensitization increases G:C to C:G transversions of *supF* gene in *Escherichia coli* mutY strain. *Mutat. Res.* **1999**, *445*, 93–98. [CrossRef] [PubMed]
3. Schulz, I.; Mahler, H.-C.; Boiteux, S.; Epe, B. Oxidative DNA base damage induced by singlet oxygen and photosensitization: Recognition by repair endonucleases and mutagenicity. *Mutat. Res.* **2000**, *461*, 145–156. [CrossRef] [PubMed]
4. Tano, K.; Iwamatsu, Y.; Yasuhira, S.; Utsumi, H.; Takimoto, K. Increased base change mutations at G:C pairs in *Escherichia coli* deficient in endonuclease III and VIII. *J. Radiat. Res.* **2001**, *42*, 409–413. [CrossRef] [PubMed]
5. Kino, K.; Miyazawa, H.; Sugiyama, H. User-friendly synthesis and photoirradiation of a flavin-linked oligomer. *Genes Environ.* **2007**, *29*, 23–28. [CrossRef]
6. Mcbride, T.J.; Schneider, J.E.; Floyd, R.A.; Loeb, L.A. Mutations induced by methylene blue plus light in single-stranded M13mp2. *Proc. Natl. Acad. Sci. USA* **1992**, *89*, 6866–6870. [CrossRef] [PubMed]
7. Ono, T.; Negishi, K.; Hayatsu, H. Spectra of superoxide-induced mutations in the lacI gene of a wild-type and a mutM strain of *Escherichia coli* K-12. *Mutat. Res.* **1995**, *326*, 175–183. [CrossRef] [PubMed]
8. Macbride, T.J.; Preston, B.D.; Loeb, L.A. Mutagenic spectrum resulting from DNA damage by oxygen radicals. *Biochemistry* **1991**, *30*, 207–213. [CrossRef]
9. Akasaka, S.; Takimoto, K. Hydrogen peroxide induces G:C to T:A and G:C to C:G transversions in the supF gene of *Escherichia coli*. *Mol. Gen. Genet.* **1994**, *243*, 500–505. [CrossRef]
10. Valentine, M.R.; Rodriguez, H.; Termini, J. Mutagenesis by peroxyradical is dominated by transversions at deoxyguanosine: Evidence for the lack of involvement of 8-oxo-dG and/or abasic site formation. *Biochemistry* **1998**, *37*, 7030–7038. [CrossRef]
11. Emmert, S.; Epe, B.; Saha-Möller, C.R.; Adam, W.; Rünger, T.M. Assessment of genotoxicity and mutagenicity of 1,2-dioxetanes in human cells using a plasmid shuttle vector. *Photochem. Photobiol.* **1995**, *61*, 136–141. [CrossRef]
12. Sargentini, N.J.; Smith, K.C. DNA sequence analysis of γ-radiation (anionic)-induced and spontaneous lacI$^d$ mutations in *Escherichia coli* K-12. *Mutat. Res.* **1994**, *309*, 147–163. [CrossRef]
13. Shin, C.Y.; Ponomareva, O.N.; Connolly, L.; Turker, M.S. A mouse kidney cell line with a G:C->C:G transversion mutator phenotype. *Mutat. Res.* **2002**, *503*, 69–76. [CrossRef]
14. Cadet, J.; Mouret, S.; Ravanat, J.-L.; Douki, T. Photoinduced damage to cellular DNA: Direct and photosensitized reactions. *Photochem. Photobiol.* **2012**, *88*, 1048–1065. [CrossRef]
15. Epe, B. DNA damage spectra induced by photosensitization. *Photochem. Photobiol. Sci.* **2012**, *11*, 98–106. [CrossRef] [PubMed]

16. Kanamori, T.; Kaneko, S.; Hamamoto, K.; Yuasa, H. Mapping the diffusion pattern of $^1O_2$ along DNA duplex by guanine photooxidation with an appended biphenyl photosensitizer. *Sci. Rep.* **2023**, *13*, 288. [CrossRef]
17. Maisuls, I.; Cabrerizo, F.M.; David-Gara, P.M.; Epe, B.; Ruiz, G.T. DNA oxidation photoinduced by norharmane rhenium(I) polypyridyl complexes: Effect of the bidentate N,N′-ligands on the damage profile. *Chem. Eur. J.* **2018**, *24*, 12902–12911. [CrossRef]
18. Hirakawa, K.; Okazaki, S.; Murakami, H.; Kanayama, N. Development of cancer-selective and effective photosensitizers through electron transfer mechanism. *J. Jpn. Soc. Laser Surg. Med.* **2021**, *41*, 349–355. [CrossRef]
19. Kawai, K.; Osakada, Y.; Fujitsuka, M.; Majima, T. Consecutive adenine sequences are potential targets in photosensitized DNA damage. *Chem. Biol.* **2005**, *12*, 1049–1054. [CrossRef]
20. Yun, B.H.; Dedon, P.C.; Geacintov, N.E.; Shafirovich, V. One-electron oxidation of a pyrenyl photosensitizer covalently attached to DNA and competition between its further oxidation and DNA hole injection. *Photochem. Photobiol.* **2010**, *86*, 563–570. [CrossRef]
21. Dumont, E.; Monari, A. Understanding DNA under oxidative stress and sensitization: The role of molecular modeling. *Front. Chem.* **2015**, *3*, 43. [CrossRef]
22. Aerssens, D.; Cadoni, E.; Tack, L.; Madder, A. A photosensitized singlet oxygen ($^1O_2$) toolbox for bio-organic applications: Tailoring $^1O_2$ generation for DNA and protein labelling, targeting and biosensing. *Molecules* **2022**, *27*, 778. [CrossRef]
23. Roberts, L.W.; Schuster, G.B. Synthesis and study of naphthacenedione (TQ) as a photosensitizer for one-electron oxidation of DNA. *Org. Lett.* **2004**, *6*, 3813–3816. [CrossRef]
24. Kino, K.; Morikawa, M.; Kobayashi, T.; Kobayashi, T.; Komori, R.; Sei, Y.; Miyazawa, H. The oxidation of 8-oxo-7,8-dihydroguanine by iodine. *Bioorg. Med. Chem. Lett.* **2010**, *20*, 3818–3820. [CrossRef]
25. Steenken, S.; Jovanovic, S.V. How easily oxidizable is DNA? One-electron reduction potentials of adenosine and guanosine radicals in aqueous solution. *J. Am. Chem. Soc.* **1997**, *119*, 397–407. [CrossRef]
26. Sugiyama, H.; Saito, I. Theoretical studies of GG-specific photocleavage of DNA via Electron Transfer: Significant lowering of ionization potential and 5′-localization of HOMO of stacked GG bases in B-form DNA. *J. Am. Chem. Soc.* **1996**, *118*, 7063–7068. [CrossRef]
27. Saito, I.; Nakamura, T.; Nakatani, K.; Yoshioka, Y.; Yamaguchi, K.; Sugiyama, H. Mapping of the hot spots for DNA damage by one-electron oxidation: Efficacy of GG doublets and GGG triplets as a trap in long-range hole migration. *J. Am. Chem. Soc.* **1998**, *120*, 12686–12687. [CrossRef]
28. Morikawa, M.; Kino, K.; Oyoshi, T.; Suzuki, M.; Kobayashi, T.; Miyazawa, H. Product analysis of photooxidation in isolated quadruplex DNA; 8-oxo-7,8-dihydroguanine and its oxidation product at 3′-G are formed instead of 2,5-diamino-4H-imidazol-4-one. *RSC Adv.* **2013**, *3*, 25694–25697. [CrossRef]
29. Morikawa, M.; Kino, K.; Oyoshi, T.; Suzuki, M.; Kobayashi, T.; Miyazawa, H. Calculation of the HOMO localization of Tetrahymena and Oxytricha telomeric quadruplex DNA. *Bioorg. Med. Chem. Lett.* **2015**, *25*, 3359–3362. [CrossRef] [PubMed]
30. Lu, R.; Nash, H.M.; Verdine, G.L. A mammalian DNA repair enzyme that excises oxidatively damaged guanines maps to a locus frequently lost in lung cancer. *Curr. Biol.* **1997**, *7*, 397–407. [CrossRef] [PubMed]
31. Maki, H.; Sekiguchi, M. MutT protein specifically hydrolyses a potent mutagenic substrate for DNA synthesis. *Nature* **1992**, *355*, 273–275. [CrossRef]
32. Brunner, S.D.; Norman, D.P.G.; Verdine, G.L. Structural basis for recognition and repair of the endogenous mutagen 8-oxoguanine in DNA. *Nature* **2000**, *403*, 859–866. [CrossRef]
33. Grollman, A.P.; Moriya, M. Mutagenesis by 8-oxoguanine: An enemy within. *Trends Genet.* **1993**, *9*, 246–249. [CrossRef] [PubMed]
34. Shibutani, S.; Takeshita, M.; Grollman, A.P. Insertion of specific bases during DNA synthesis past the oxidation-damaged base 8-oxodG. *Nature* **1991**, *349*, 431–434. [CrossRef] [PubMed]
35. Lipscomb, L.A.; Peek, M.E.; Morningstar, M.L.; Verghis, S.M.; Miller, E.M.; Rich, A.; Essigmann, J.M.; Williams, L.D. X-ray structure of a DNA decamer containing 7,8-dihydro-8-oxoguanine. *Proc. Natl. Acad. Sci. USA* **1995**, *92*, 719–723. [CrossRef] [PubMed]
36. Moriya, M. Single-stranded shuttle phagemid for mutagenesis studies in mammalian cells: 8-Oxoguanine in DNA induces targeted G:C->T:A transversions in simian kidney cells. *Proc. Natl. Acad. Sci. USA* **1993**, *90*, 1122–1126. [CrossRef] [PubMed]
37. Cadet, J.; Berger, M.; Buchko, G.W.; Joshi, P.C.; Raoul, S.; Ravanat, J.-L. 2,2-Diamino-4-[(3,5-di-O-acetyl-2-deoxy-L-D-erythro-pentofuranosyl)amino]-5-(2H)-oxazolone: A novel and predominant radical oxidation product of 3,5-di-O-acetyl-2-deoxyguanosine. *J. Am. Chem. Soc.* **1994**, *116*, 7403–7404. [CrossRef]
38. Raoul, S.; Berger, M.; Buchko, G.W.; Joshi, P.C.; Morin, B.; Weinfeld, M.; Cadet, J. $^1H$, $^{13}C$ and $^{15}N$ Nuclear magnetic resonance analysis and chemical features of the two main radical oxidation products of 2-deoxyguanosine: Oxazolone and imidazolone nucleosides. *J. Chem. Soc. Perkin Trans.* **1996**, *2*, 371–381. [CrossRef]
39. Duarte, V.; Muller, J.G.; Burrows, C.J. Insertion of dGMP and dAMP during in vitro DNA synthesis opposite an oxidized form of 7,8-dihydro-8-oxoguanine. *Nucleic Acids Res.* **1999**, *27*, 496–502. [CrossRef]
40. Leipold, M.D.; Muller, J.G.; Burrows, C.J.; David, S.S. Removal of hydantoin products of 8-oxoguanine oxidation by the *Escherichia coli*. *Biochemistry* **2000**, *39*, 14984–14992. [CrossRef]
41. Luo, W.; Muller, J.G.; Rachlin, E.M.; Burrows, C.J. Characterization of spiroiminodihydantoin as a product of one-electron oxidation of 8-oxo-7,8-dihydroguanosine. *Org. Lett.* **2000**, *2*, 613–616. [CrossRef]
42. Kino, K.; Sugiyama, H. Possible cause of G-C-->C-G transversion mutation by guanine oxidation product, imidazolone. *Chem. Biol.* **2001**, *8*, 369–378. [CrossRef]

43. Neeley, W.L.; Delaney, J.C.; Henderson, P.T.; Essigmann, J.M. In vivo bypass efficiencies and mutational signatures of the guanine oxidation products 2-aminoimidazolone and 5-guanidino-4-nitroimidazole. *J. Biol. Chem.* **2004**, *279*, 43568–43573. [CrossRef] [PubMed]
44. Kino, K.; Sugasawa, K.; Mizuno, T.; Bando, T.; Sugiyama, H.; Akita, M.; Miyazawa, H.; Hanaoka, F. Eukaryotic DNA polymerases α, β and ε incorporate guanine opposite 2,2,4-triamino-5(2H)-oxazolone. *ChemBioChem* **2009**, *10*, 2613–2616. [CrossRef] [PubMed]
45. Suzuki, M.; Kino, K.; Kawada, T.; Morikawa, M.; Kobayashi, T.; Miyazawa, H. Analysis of nucleotide insertion opposite 2,2,4-triamino-5(2H)-oxazolone by eukaryotic B- and Y-family DNA polymerases. *Chem. Res. Toxicol.* **2015**, *28*, 1307–1316. [CrossRef]
46. Kornyushyna, O.; Berges, A.M.; Muller, J.G.; Burrows, C.J. In vitro nucleotide misinsertion opposite the oxidized guanosine lesions spiroiminodihydantoin and guanidinohydantoin and DNA synthesis past the lesions using *Escherichia coli* DNA polymerase I (Klenow Fragment). *Biochemistry* **2002**, *41*, 15304–15314. [CrossRef]
47. Henderson, P.T.; Delaney, J.C.; Muller, J.G.; Neeley, W.L.; Tannenbaum, S.R.; Burrows, C.J.; Essigmann, J.M. The hydantoin lesions formed from oxidation of 7,8-dihydro-8-oxoguanine are potent sources of replication errors in vivo. *Biochemistry* **2003**, *42*, 9257–9262. [CrossRef]
48. Neeley, W.L.; Delaney, S.; Alekseyev, Y.O.; Jarosz, D.F.; Delaney, J.C.; Walker, G.C.; Essigmann, J.M. DNA polymerase V allows bypass of toxic guanine oxidation products in vivo. *J. Biol. Chem.* **2007**, *282*, 12741–12748. [CrossRef]
49. Delaney, S.; Neeley, W.L.; Delaney, J.C.; Essigmann, J.M. The substrate specificity of MutY for hyperoxidized guanine lesions in vivo. *Biochemistry* **2007**, *46*, 1448–1455. [CrossRef] [PubMed]
50. Kino, K.; Kawada, T.; Hirao-Suzuki, M.; Morikawa, M.; Miyazawa, H. Products of oxidative guanine damage form base pairs with guanine. *Int. J. Mol. Sci.* **2020**, *21*, 7645. [CrossRef]
51. McNally, A.; Prier, C.K.; MacMillan, D.W.C. Discovery of an α-amino C-H arylation reaction using the strategy of accelerated serendipity. *Science* **2011**, *334*, 1114–1117. [CrossRef] [PubMed]
52. Kim, D.K.; Dong, V.M. An enlightening reactor. *ACS Cent. Sci.* **2017**, *3*, 526. [CrossRef]
53. Lin, S.; Ischay, M.A.; Fry, C.G.; Yoon, T.P. Radical cation Diels-Alder cycloadditions by visible light photocatalysis. *J. Am. Chem. Soc.* **2011**, *133*, 19350–19353. [CrossRef]
54. DiRocco, D.A.; Dykstra, K.; Krska, S.; Vachal, P.; Conway, D.V.; Tudge, M. Late-stage functionalization of biologically active heterocycles through photoredox catalysis. *Angew. Chem. Int. Ed.* **2014**, *53*, 4802–4806. [CrossRef]
55. Ito, E.; Fukushima, T.; Kawakami, T.; Murakami, K.; Itami, K. Catalytic dehydrogenative C-H imitation of arenas enabled by photo-generated hole donation to sulfonimide. *Chem.* **2017**, *2*, 383–392. [CrossRef]
56. Zeitler, K. Photoredox catalysis with visible light. *Angew. Chem. Int. Ed.* **2009**, *48*, 9757–9987. [CrossRef]
57. Patel, S.C.; Burns, N.Z. Conversion of aryl azides to aminopyridines. *J. Am. Chem. Soc.* **2022**, *144*, 17797–17802. [CrossRef]
58. Woo, J.; Stein, C.; Christian, A.H.; Levin, M.D. Carbon-to-nitrogen single-atom transmutation of azaarenes. *Nature* **2023**, *623*, 77–82. [CrossRef]
59. Kino, K.; Kobayashi, T.; Arima, E.; Komori, R.; Kobayashi, T.; Miyazawa, H. Photoirradiation products of flavin derivatives, and the effects of photooxidation on guanine. *Bioorg. Med. Chem. Lett.* **2009**, *19*, 2070–2074. [CrossRef] [PubMed]
60. Kino, K.; Nakatsuma, A.; Nochi, H.; Kiriyama, Y.; Kurita, T.; Kobayashi, T.; Miyazawa, H. Commentary on the phototoxicity and absorption of vitamin $B_2$ and its degradation product, lumichrome. *Pharm. Anal. Acta* **2015**, *6*, 403.
61. Ahmad, I.; Vaid, F.H.M. *Flavins: Photochemistry and Photobilogy*; Silva, E., Edwards, A.M., Eds.; RSC Publishing: Cambridge, UK, 2006; pp. 13–40.
62. Posthuma, J.; Berends, W. Energy transfer in aqueous solution. *Biochim. Biophys. Acta* **1966**, *112*, 422–435. [CrossRef] [PubMed]
63. Penzer, G.R.; Radda, G.K. The chemistry and biological function of isoalloxazines (flavines). *Q. Rev. Chem. Soc.* **1967**, *21*, 43–65. [CrossRef]
64. Gore, D.M.; Margineanu, A.; French, P.; O'Brart, D.; Dunsby, C.; Allan, B.D. Two-photon fluorescence microscopy of corneal riboflavin absorption. *Investig. Ophthalmol. Vis. Sci.* **2014**, *55*, 2476–2481. [CrossRef]
65. Zhang, Y.; Sukthankar, P.; Tomich, J.M.; Conrad, G.W. Effect of the synthetic NC-1059 peptide on diffusion of riboflavin across an intact corneal epithelium. *Investig. Ophthalmol. Vis. Sci.* **2012**, *53*, 2620–2629. [CrossRef] [PubMed]
66. Thakuri, P.S.; Joshi, R.; Basnet, S.; Pandey, S.; Taujale, S.D.; Mishra, N. Antibacterial photodynamic therapy on staphylococcus aureus and pseudomonas aeruginosa in-vitro. *Nepal. Med. Coll. J.* **2011**, *13*, 281–284. [PubMed]
67. de Jesus, M.B.; Fraceto, L.F.; Martini, M.F.; Pickholz, M.; Ferreira, C.V.; de Paula, E. Non-inclusion complexes between riboflavin and cyclodextrins. *J. Pharm. Pharmacol.* **2012**, *64*, 832–842. [CrossRef] [PubMed]
68. Yamabe, S.; Tsuchida, N.; Yamazaki, S. A DFT study on the degradation mechanism of vitamin $B_2$. *Food Chem. Mol. Sci.* **2022**, *4*, 100080. [CrossRef] [PubMed]
69. Ahmad, I.; Abbas, S.H.; Anwar, Z.; Sheraz, M.A.; Ahmed, S.; Arsalan, A.; Bano, R. Stability-indicating photochemical method for the assay of riboflavin: Lumichrome Method. *J. Chem.* **2015**, *2015*, 256087. [CrossRef]
70. Sheraz, M.A.; Kazi, S.H.; Ahmed, S.; Anwar, Z.; Ahmad, I. Photo, thermal and chemical degradation of riboflavin. *Beilstein J. Org. Chem.* **2014**, *10*, 1999–2012. [CrossRef]
71. Sheraz, M.; Kazi, S.; Ahmed, S.; Qadeer, K.; Khan, M.; Ahmad, I. Multicomponent spectrometric analysis of riboflavin and photoproducts and their kinetic applications. *Open Chem.* **2014**, *12*, 635–642. [CrossRef]

72. McCormick, D.B. *Present Knowledge in Nutrition*, 10th ed.; Erdman, J.W., Macdonald, I.A., Zeisel, S.H., Eds.; International Life Sciences Institute: Washington, DC, USA, 2012; pp. 280–292.
73. Chaudhuri, S.; Batabyal, S.; Polley, N.; Pal, S.K. Vitamin $B_2$ in nanoscopic environments under visible light: Photosensitized antioxidant or phototoxic drug? *J. Phys. Chem. A* **2014**, *118*, 3934–3943. [CrossRef] [PubMed]
74. Remucal, C.K.; McNeill, K. Photosensitized amino acid degradation in the presence of riboflavin and its derivatives. *Environ. Sci. Technol.* **2011**, *45*, 5230–5237. [CrossRef] [PubMed]